



UNIVERSITY OF LEEDS

This is a repository copy of *Diblock Copolymer Micelles and Supported Films with Noncovalently Incorporated Chromophores: A Modular Platform for Efficient Energy Transfer*.

White Rose Research Online URL for this paper:  
<http://eprints.whiterose.ac.uk/87782/>

Version: Accepted Version

---

**Article:**

Adams, PG [orcid.org/0000-0002-3940-8770](http://orcid.org/0000-0002-3940-8770), Collins, AM, Sahin, T et al. (7 more authors) (2015) Diblock Copolymer Micelles and Supported Films with Noncovalently Incorporated Chromophores: A Modular Platform for Efficient Energy Transfer. *Nano Letters*, 15 (4). pp. 2422-2428. ISSN 1530-6984

<https://doi.org/10.1021/nl504814x>

---

**Reuse**

Items deposited in White Rose Research Online are protected by copyright, with all rights reserved unless indicated otherwise. They may be downloaded and/or printed for private study, or other acts as permitted by national copyright laws. The publisher or other rights holders may allow further reproduction and re-use of the full text version. This is indicated by the licence information on the White Rose Research Online record for the item.

**Takedown**

If you consider content in White Rose Research Online to be in breach of UK law, please notify us by emailing [eprints@whiterose.ac.uk](mailto:eprints@whiterose.ac.uk) including the URL of the record and the reason for the withdrawal request.



[eprints@whiterose.ac.uk](mailto:eprints@whiterose.ac.uk)  
<https://eprints.whiterose.ac.uk/>

Diblock copolymer micelles and supported films with non-covalently  
incorporated chromophores: a modular platform for efficient energy  
transfer

*Peter G. Adams,<sup>†,1,2</sup> Aaron M. Collins,<sup>†,1</sup> Tuba Sahin,<sup>‡</sup> Vijaya Subramanian,<sup>§</sup> Volker S. Urban,<sup>+</sup>  
Pothiappan Vairaprakash,<sup>‡</sup> Yongming Tian,<sup>†,1</sup> Deborah G. Evans,<sup>§</sup> Andrew P. Shreve,<sup>§,\*</sup> Gabriel  
A. Montaño<sup>†,\*</sup>*

<sup>†</sup>Center for Integrated Nanotechnologies, Los Alamos National Laboratories, Los Alamos, NM,  
87545; <sup>‡</sup>Department of Chemistry, North Carolina State University, Raleigh, NC, 27695; <sup>§</sup>Center  
for Biomedical Engineering, University of New Mexico, Albuquerque, NM, 87131; <sup>+</sup>Biology  
and Soft Matter Division, Oak Ridge National Laboratory, Oak Ridge, Tennessee 37831;  
<sup>1</sup>Department of Chemistry, New Mexico Institute of Mining and Technology, Socorro, NM  
87801.

<sup>1</sup> These authors contributed equally to this work

<sup>2</sup> Current address: School of Physics and Astronomy, University of Leeds, Leeds LS2 9JT,  
United Kingdom

\* To whom correspondence should be addressed: [gbmon@lanl.gov](mailto:gbmon@lanl.gov), [shreve@unm.edu](mailto:shreve@unm.edu)

**ABSTRACT:**

We report generation of modular, artificial light-harvesting assemblies where an amphiphilic diblock copolymer, poly(ethylene oxide)-*block*-poly(butadiene), serves as the framework for non-covalent organization of BODIPY-based energy donor and bacteriochlorin-based energy acceptor chromophores. The assemblies are adaptive, forming well-defined micelles in aqueous solution and high-quality monolayer and bilayer films on solid supports, with the latter showing greater than 90% energy transfer efficiency. This study lays the groundwork for further development of modular, polymer-based materials for light harvesting and other photonic applications.

**KEYWORDS:**

Amphiphilic diblock copolymers, artificial light harvesting , Förster resonance energy transfer,

**TEXT:**

Biological light-harvesting systems allow for efficient trapping of solar energy in a cellular environment,<sup>1-3</sup> but these properties do not always translate to effective engineered biomaterials for practical applications. Ideally, artificial light-harvesting (LH) approaches would build upon the desirable attributes of natural photosynthetic systems to provide functional materials that have adaptable responses, are inexpensive to manufacture, are amenable to large-scale assembly, allow controlled modulation of solar conversion efficiency, have extensive and

flexible spectral coverage (ability to incorporate a variety of chromophores), and can be integrated with various substrates or fabricated materials for energy collection. In this work, we show that these properties can be achieved through the use of amphiphilic diblock co-polymers as a flexible matrix for organization of donor and acceptor chromophores.

Two major approaches to the creation of artificial light-harvesting systems have involved either the adaptation of biological systems or the chemical synthesis of new supramolecular constructs that mimic biological systems in structure or function. Synthetic biology approaches have been used to redesign existing LH proteins<sup>4-6</sup> or to design entirely new peptides<sup>7, 8</sup> for enhanced function. Alternatively, chemical synthesis has been used to generate novel multi-component organic molecules, comprised of covalently linked chromophores and electron-active materials, such as metal nanoparticles, fullerenes<sup>9</sup> and dendrimers.<sup>10, 11</sup> Both proteins and synthetic organic molecules share some of the same limitations, including limited modularity (specific structure and chromophore binding) and a design, synthesis and purification process that is complex, labor-intensive, and expensive. From these considerations, we are motivated to design a nanomaterial-based modular system that will allow straightforward incorporation of various cofactors, and demonstrate these materials as a new platform for future functional devices.

An alternative approach for developing novel LH materials is to dispense with protein scaffolds or complex organic molecules and design a modular matrix to assemble chromophores (or other cofactors). Amphiphilic diblock copolymers represent an attractive alternative framework for the design of bio-inspired LH systems. Some advantages of synthetic polymers include: facile chemical synthesis, commercial availability, ability to functionalize, propensity for self-assembly, higher stability, and tunable responses to external stimuli.<sup>16</sup> Polymeric

assemblies have been successfully exploited for drug delivery,<sup>17</sup> in optical biosensors,<sup>18</sup> and as photoluminescent systems.<sup>19</sup> We emphasize that polymers could allow greater modularity for biomimetic light harvesting, as the process of polymer self-assembly is spontaneous and achieved by non-covalent associations, allowing the potential for interchangeable incorporation of a myriad of different cofactors. Previously, diblock copolymers have been used to encapsulate and spatially organize chromophores under certain conditions, revealing the potential for controlling energy transfer processes.<sup>20</sup> Thin films of segregated polymer micelles with different combinations of chromophores and other cofactors were designed with multiple defined emission bands.<sup>21,22</sup> However, these film relied upon spin-coating polymer/chromophore micelles from organic solvents. We wished to explore polymeric LH assemblies under more biologically relevant aqueous conditions.

Poly(ethylene oxide)-*block*-poly(butadiene) (PEO-*b*-PBD) (Figure 1A) is an amphiphilic block copolymer that self-assembles into a variety of conformations dependent on the block/block length, polymer concentration, solvent quality and environmental conditions.<sup>23-25</sup> Hydrophobic fluorescent dyes and quantum dots have previously been incorporated into long-chain vesicle-forming PEO-*b*-PBD, showing the potential for ‘hydrophobic loading’.<sup>26</sup> Recently, a 1.3/1.2 kDa (block/block ratio) PEO-*b*-PBD copolymer was extensively characterized<sup>27</sup> as forming micelles in aqueous solution but reorganizing into bilayer films of similar scale to lipid bilayers when deposited onto hydrophilic surfaces and monolayer films on hydrophobic surfaces. In all cases, the hydrophobic PBD block was sequestered and the hydrophilic PEO block exposed to the aqueous solvent, analogous to lipid arrangements, leading to its description as a biomimetic polymer<sup>27</sup> and making it an interesting candidate for further application. In the

current study, we investigate the use of this PEO-*b*-PBD as a matrix to organize chromophores in a non-covalent manner for building polymeric LH nanocomposites.

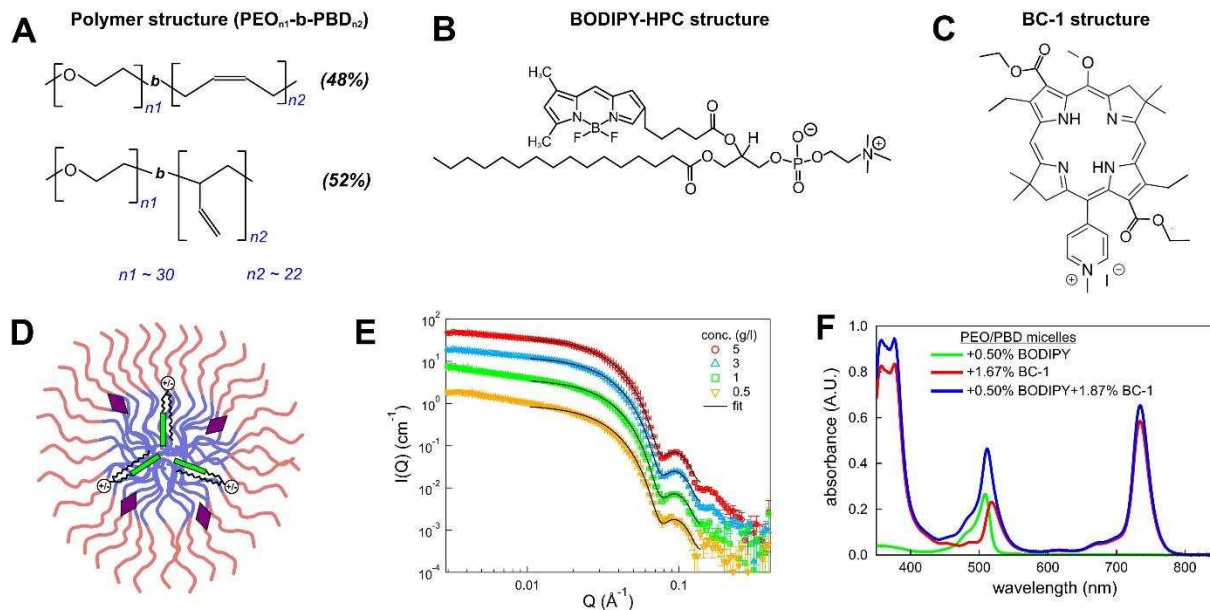


**Figure 1. Chemical structures and design of polymer-chromophore nanocomposites.** Chemical structures of (A) the PEO-*b*-PBD polymer, (B) the BODIPY-HPC donor chromophore, and (C) the BC-1 acceptor chromophore. (D) Schematic of the proposed chromophore arrangement in the polymer micelle (PEO, red; PBD, blue; BC-1, purple diamond; BODIPY, green). (E) SANS showing scattering data from a concentration range of PEO-*b*-PBD micelles, fitted to a spherical core-shell model. (F) Absorbance spectra of three representative polymer-chromophore preparations.

A BODIPY chromophore was chosen as the excitation ‘donor’ for its favorable stability, hydrophobic character, low tendency to self-aggregate, high extinction coefficient, high fluorescence quantum yield and relatively sharp emission band.<sup>28</sup> We used an analog of BODIPY FL attached through a C<sub>5</sub>-fatty acyl chain to a phosphocholine lipid to direct its assembly, termed “BODIPY-HPC” (Figure 1B). For the acceptor, a new bacteriochlorin was synthesized, termed “BC-1” (originally, BC-MePy15)<sup>29</sup> (Figure 1C). This compound was designed to have excellent spectral overlap with BODIPY to allow high efficiency of Förster Resonance Energy Transfer (FRET), and amphiphilic character to promote its location within polymer micelles, as discussed below.

Polymer/chromophore nanocomposites were assembled by dissolving the polymer and pigments in tetrahydrofuran (THF) in the ratio desired for each particular preparation. THF is a suitable co-solvent for all components of the LH system (PEO-*b*-PBD, BODIPY-HPC and BC-1) and, importantly, one that is miscible with water. The solvent quality was then changed by the gradual injection of water, followed by rotary evaporation to remove the THF. As the proportion of water to THF increases, micellization of the polymer occurs spontaneously as it becomes thermodynamically favorable for polymers to cluster into small aggregates that bury the hydrophobic PBD and incorporate both chromophores. The hydrophobic nature of BODIPY favors its segregation to the hydrophobic core of the micelle, but due to its tethering to the amphiphilic (HPC) lipid, the BODIPY moiety is expected to be in close proximity to the block/block interface (<1 nm, approximate length of lipid tail). Amphiphilic BC-1 is expected to be positioned at the hydrophilic/hydrophobic interface of the polymer. In a polar solvent, such as water, one thus anticipates an arrangement for the chromophores within the polymer micelle similar to that shown in Figure 1D.

Dynamic light scattering (DLS) revealed that the predominant particles in our preparations were ~20 nm in outer diameter (Figure S1A and B in the Supporting Information), concurrent with previous reports.<sup>27</sup> Static light scattering data supported the presence of a predominantly micellar solution and allowed calculation of an approximate micelle aggregation number of ~225 (Section 1 in the Supporting Information), consistent with values for other amphiphilic diblock copolymer micelles of similar block lengths.<sup>30</sup> Small Angle Neutron Scattering (SANS) data (Figure 1E) of the polymer preparations allowed a more detailed description of the polymer system. The data could not be fitted to simple shapes with homogenous scattering length density such as a solid sphere, ellipsoid or cylinder, rather, a spherical core-shell model with a compact core and a loose corona containing a high concentration of water provided the best fit (for further details, see Supporting Information, Section 1). This analysis revealed micelles with an outer diameter of 18.0 nm, in good agreement with DLS, and a diameter of 11.4 nm for the PBD core. Absorbance spectra are displayed in Figure 1F for representative micelle preparations containing either BODIPY-HPC, BC-1 or a mixture of both. The bands observed in these spectra are very similar to those for the chromophores in THF (Figure S3 in the Supporting Information), indicating that incorporation into the polymer micelles preserved their monomeric optical properties. In contrast, if the polymer was omitted, broadened absorption bands and low fluorescence emission was observed after exchange to water, suggesting chromophore aggregation, showing the necessity of a polymer scaffold.

We found that PEO-*b*-PBD/chromophore nanocomposites could be assembled with any donor or acceptor concentration up to ~3% (chromophore mol% relative to polymer concentration) before chromophore aggregation effects were observed. Therefore, for detailed

characterization, we generated sets of samples at chromophore concentrations that exhibited good energy transfer (10-60% efficiency) and no observed aggregation. Set 1 had a range of acceptor concentrations (0-2.13% BC-1) at a relatively constant donor concentration (~0.5% BODIPY-HPC); Set 2 had a range of donor concentrations (0-0.91% BODIPY-HPC) at a constant acceptor concentration (~0.8% BC-1). Samples from each set were prepared in parallel and then immediately characterized by absorbance, steady-state and time-resolved fluorescence spectroscopies. Spectral analysis of absorbance data allowed quantification of the relative chromophore concentrations in the final product of each individual preparation (see Section 3 and Figure S4A-B in the Supporting Information).

Steady-state and time-resolved fluorescence spectroscopies were used as independent methods to assess energy-transfer efficiencies within the assemblies (Figure 2; for a more extensive dataset see Figure S5 and S6 in the Supporting Information). Increased quenching of donor fluorescence emission was observed in sample Set 1 with increasing acceptor concentration at a constant donor concentration (Figure 2A). Conversely, enhanced acceptor emission was observed in Set 2 with increasing donor concentration at a constant acceptor concentration (Figure 2B). Both observations are highly indicative of donor-acceptor energy transfer. These graphs clearly show these trends in a qualitative manner, but for a more accurate quantitative comparison of the ensemble donor-acceptor energy-transfer efficiency (ETE), we performed graphical analysis of the data (as described in Section 3 and Figure S4C in the Supporting Information). Briefly, the ETE was calculated from integrated fluorescence intensity of the donor from 480–650 nm, in presence ( $F_{DA}$ ) or absence ( $F_D$ ) of acceptor, using the conventional relationship for FRET<sup>31</sup>:

$$ETE = 1 - \frac{F_{DA}}{F_D} \quad (1)$$

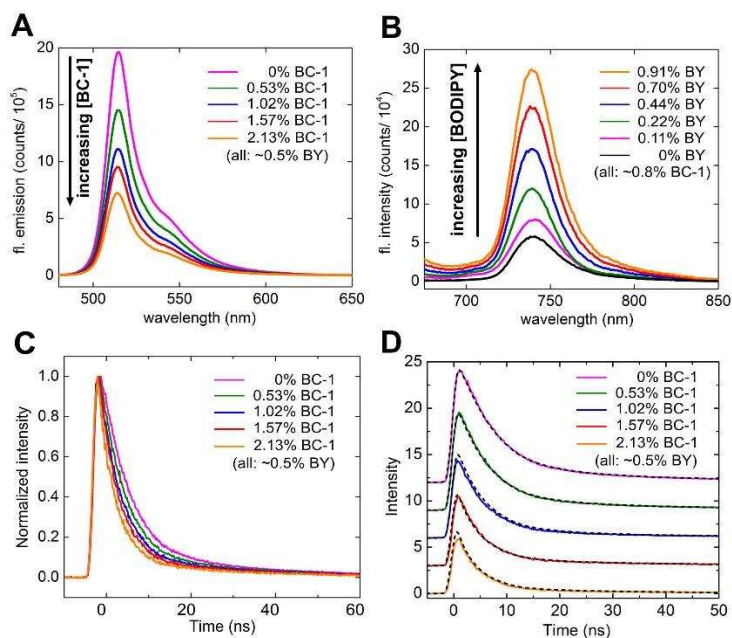


**Figure 2. Spectroscopic characterization of the polymer-chromophore micelles.** (A) Steady-state fluorescence emission spectra from BODIPY (excitation at 469 nm) from polymer/chromophore micelle samples in Set 1. (B) Steady-state fluorescence emission spectra of the BC-1 peak (excitation at 469 nm) from sample Set 2. Legend shows BODIPY-HPC concentration (“% BY”) and BC-1 concentration (“% BC-1”) in each sample. (C) Intensity normalized decay curves of BODIPY fluorescence in polymer/chromophore micelle samples from Set 1. Excitation was provided by a 465 nm LED and emission collected at 514 nm (12 nm bandwidth). (D) Decay curves from experimental data (solid lines) plotted with decay curves generated from theoretical model convolved with an instrument response function (dashed lines). Spectra and fits present actual relative amplitudes (i.e., not normalized to the same peak intensity), and are offset in the y-direction (for clarity).

The results show that ETE increases non-linearly with acceptor concentration, as displayed graphically in Figure 3 and discussed later (raw data is shown in Tables S1 and S2 in the Supporting Information). Analysis of fluorescence decay curves (time-resolved fluorescence data) was used as an independent method to assess ETE. A clear trend was observed from normalized curves whereby the rate of decay of the donor fluorescence increased (i.e. decreased fluorescence lifetime) with increasing BC-1 (acceptor) concentration (Figure 2C). This result indicated that a faster process occurred as acceptor concentration increased, corresponding to a faster decay of the fluorescence signal, in agreement with the steady-state FRET data. In contrast, no change was observed in the fluorescence decay curves with increasing BODIPY-HPC concentration at constant acceptor concentration (Figure S6B in the Supporting Information).

A theoretical model of our polymer system was developed based on Förster theory of energy transfer<sup>32</sup> and the measured structural and optical properties of the polymer-chromophore system (chromophore concentration, polymer aggregation number and core diameter, Förster radius; for further detail on the model see Section 5 of Supplemental Information). This approach was used to independently model donor fluorescence decay taking into account FRET to a randomly distributed set of acceptors within each micelle. The acceptors are assumed to be distributed uniformly on the surface of a sphere corresponding to the PBD core of the micelle. These theoretical decay curves as a function of increasing average acceptor concentration are in good agreement with the experimental data in both shape and amplitude (Figure 2D).

Plotting the ETE against acceptor concentration shows a clear trend (Figure 3, *blue data points*) where ETE increases with the BC-1 (acceptor) concentration. The theoretical model of

the polymer system described above was also used to independently predict the ETE for a range of acceptor concentrations and plotted as a dashed line on the graph.

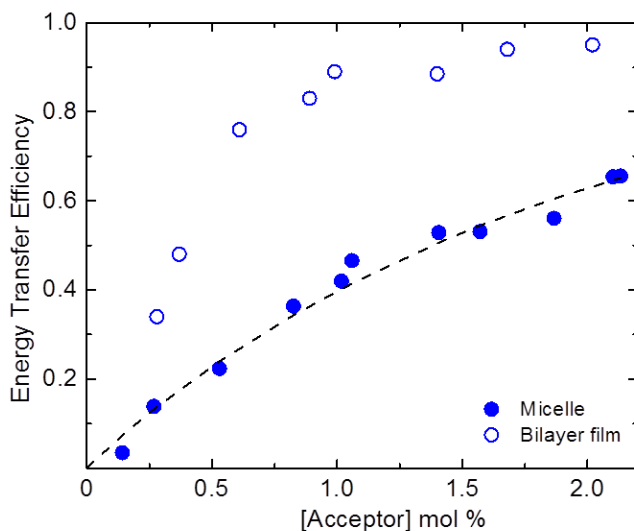


**Figure 3. Energy-transfer efficiency of polymer/chromophore nanocomposites.** ETE for polymer micelles from Set 1 (blue circles) and as bilayer films (open blue circles) plotted against the acceptor BC-1 concentration (constant BODIPY-HPC ~0.5%). The dashed line represents the theoretical model of FRET in the polymer micelles (see materials and methods).

The excellent fit between experimental data and the theoretical model shows that PEO-*b*-PBD/chromophore nanocomposites demonstrate reproducible energy transfer that follows simple Förster theory for uniformly distributed chromophores. Note, ETE is independent of the BODIPY-HPC (donor) concentration (at constant BC-1 concentration, see Figure S7 in the Supporting Information), consistent with Förster theory for independently acting donor molecules<sup>32</sup>. These results demonstrate that a polymer micelle-based system for independent, non-interacting, chromophores has the ability to harvest energy in a predictable manner, an important indication that more advanced polymeric LH systems could be rationally designed.

We wished to compare the solution-based LH system (i.e. aqueous micelles) to a solid-supported thin film system. The motivation for this comparison is two-fold. First, most natural LH systems occur in membranes, so understanding energy flow in two dimensions provides an important point of comparison to natural systems. Second, ultimately, there is interest in coupling light-harvesting systems to energy-transducing surfaces, so investigation of thin-film geometries provides a step in that direction. We took advantage of the ability of PEO-*b*-PBD to form well-defined bilayer films on hydrophilic surfaces and monolayers on hydrophobic surfaces<sup>27</sup>. PEO-*b*-PBD/chromophore micelle samples with a range of BC-1 concentrations (0-2.0%) and similar BODIPY-HPC concentration (~0.5%) were deposited onto hydrophilic glass substrates to form surface-supported bilayer films and characterized (under liquid) using laser-scanning confocal microscopy (LSCM) and atomic force microscopy (AFM). LSCM images of BODIPY fluorescence showed a homogenous distribution over hundreds of microns (Figure 4A-D, panels '*before*'), and AFM revealed a continuous, flat surface (Figure 4F), confirming that polymer films were of high quality.

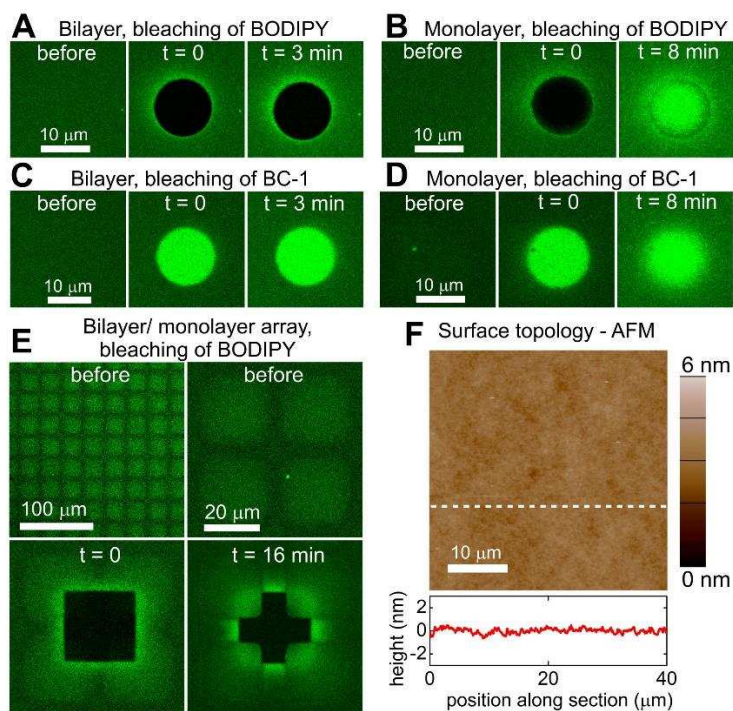


**Figure 4. Energy transfer and chromophore mobility in supported polymer bilayers and monolayers.** (A)-(E) LSCM images showing fluorescence recovery after photobleaching (FRAP) experiments. Only the fluorescence from BODIPY is visualized, but the effect of bleaching BC-1 can be inferred. Polymer bilayers in (A), (C) and polymer monolayers in (B), (D) were formed by deposition of PEO-*b*-PBD micelles onto hydrophilic (piranha-cleaned) or hydrophobic (silanized) glass substrates respectively; the arrays of alternating polymer monolayers/ bilayers in (E) were generated by deposition of micelles onto a patterned substrate generated by microcontact printing (see Methods in Supporting Information). BODIPY was preferentially bleached in (A) and (B) by using a 488 nm laser, whereas BC-1 was preferentially bleached in (C) and (D) using a 543 nm laser. Images were acquired before, immediately after ( $t = 0$ ) and a defined period after photobleaching ( $t = x$  min), as shown. All images with one FRAP series are displayed at the same intensity color scale, but scales differ between samples to provide optimum image contrast. (F) AFM topograph of a representative polymer bilayer film, imaged under buffer. Below, a height profile displays the height data across the white-dashed line in the image. The surface topography deviates by < 1 nm over the 40  $\mu\text{m}$  field.

ETE for polymer bilayers was calculated from the mean fluorescence counts in LSCM images, using Eqn. 1 (see Figure 3, blue open circles, and Table S3 in the Supporting Information). ETE was significantly greater for chromophores within polymer bilayers compared to micelles, and reached values up to 0.95 (Figure 3). This effect is likely related to the change in conformation of polymers as they interact with the substrate, as compared to their aqueous environment. As described here and previously by Goertz and coworkers,<sup>27</sup> PEO-*b*-PBD micelles have a diameter of ~20 nm, whereas PEO-*b*-PBD bilayers are a mere 5 nm in thickness. The tighter packing of polymer chains in a bilayer compared to micelles should also result in a higher density of chromophores and corresponding decreased donor-acceptor separations, resulting in the observed enhanced ETE. By contrast, this effect was not observed in a lipid-based system containing BODIPY-HPC and BC-1 for which solution-based lipid vesicles had comparable ETE to supported lipid bilayers (see Table S4 in the Supporting Information). The lipid studies compare two types of bilayers, vesicles and substrate-supported membranes, where large scale reorganization of the amphiphilic matrix is not expected. In contrast, the polymer results suggest that changes in the nature of the polymer between micelles in solution and bilayers on surfaces can lead to large changes in the separation distances of embedded molecules. These experiments demonstrate the flexible, responsive nature of PEO-*b*-PBD-based optical nanomaterials.

The fluidity of the polymer films was tested by fluorescence recovery after photobleaching (FRAP) experiments. Previous FRAP studies have shown that PEO-*b*-PBD bilayers are ‘immobile’, with no recovery of embedded lipid dyes, whereas lipid dyes in PEO-*b*-PBD monolayers have lateral mobility comparable to the same dye in lipid membranes.<sup>27</sup> These mobility patterns for BODIPY-HPC in bilayer and monolayer samples were also observed in the

current study, but with an additional interesting optical response due to the presence or absence of the BC-1 acceptor. For polymer bilayers, bleaching of BODIPY led to no FRAP recovery (Figure 4A), as expected, however, preferential bleaching of BC-1 caused an increased BODIPY fluorescence intensity in the ‘bleach region’ (Figure 4C). This result can be rationalized as follows: initially the BODIPY emission is quenched by active BC-1 (due to energy transfer), but after BC-1 acceptor is bleached it no longer quenches BODIPY leading to an increase in the relative intensity of BODIPY emission. The enhanced region remained a constant shape for many minutes after bleaching indicating that BC-1 is immobile. For polymer monolayers, we observed a relative difference in the mobility of the BODIPY and BC-1. After preferential BODIPY bleaching in polymer monolayers, there is recovery of its fluorescence not merely to the original intensity but to an enhanced intensity relative to the surrounding area (Figure 4B). This result suggests that, while the 488 laser preferentially bleaches the BODIPY chromophore, some BC-1 chromophores are also bleached (consistent with the absorbance spectra of the two dyes, Figure 1G). Following the bleaching, ‘fresh’ BODIPY-HPC diffuses into the bleach region but the BC-1 remains relatively static, leading to reduced donor quenching in this region. Preferential bleaching of BC-1 in polymer monolayers also causes an enhancement of BODIPY fluorescence, as for polymer bilayers (Figure 4D), but a gradual blurring of the shape of the enhanced region shows that the BC-1 does have limited, albeit relatively low mobility. To allow side-by-side comparison of the monolayer/bilayer polymer morphology, we performed FRAP on an array pattern of alternating PEO-*b*-PBD monolayers and bilayers (Figure 4E). After the photobleaching at 488 nm of a square region spanning bilayers (*grid*) and monolayers (*boxes*), excellent BODIPY recovery is observed in the monolayers leading to an effective ‘enhanced’ fluorescence, while no recovery is observed in bilayers and a bleached “+” shape remains,

surrounded by a brighter halo. Our data on differential chromophore mobility in solid-supported polymer films illustrates another aspect of the versatility of polymers in creating a functional surface with the potential for designing spatially patterned variable optical responses.

We have demonstrated high efficiency energy transfer in an aqueous, biomimetic polymer assemblies, for the first time, as a proof-of-concept. Our experimentally measured ETE closely follows that predicted from models that follow Förster theory applied to randomly distributed, non-interacting chromophores, providing validation of experimental results and also suggesting that more complex energy transfer assemblies could be rationally designed. Below, we briefly discuss the relevance of our polymer-based LH system, in contrast to biological LH systems, and discuss the potential applications of novel polymer-based biomaterials.

Artificial photosynthetic systems have been previously demonstrated in studies using BODIPY as a donor for energy transfer (e.g. to bacterial RC proteins) or as an electron donor (e.g. to fullerenes).<sup>28</sup> While natural LH systems typically rely upon intricate organization of chromophores to direct energy and electron transfers,<sup>33</sup> our system is designed to be much simpler with a self-assembly process that does not require proteins or complex organic synthesis, but instead relies upon incorporation of cofactors into assemblies of amphiphilic polymers. Natural LH pigment-protein complexes have high affinity binding sites which are specific for a defined cofactor.<sup>33</sup> In contrast, the polymer-driven assembly process allows modularity, with the potential for incorporation of practically any desired hydrophobic or amphiphilic cofactor into the same basic architecture. Future applications of polymer-based LH nanocomposites could also allow the non-covalent incorporation of biological electron carriers,<sup>34</sup> or carbon nanomaterials such as fullerenes<sup>35, 36</sup> or carbon nanotubes<sup>37</sup>, allowing electron-active assemblies and new functional devices.

Photosynthetic membranes are highly responsive, often changing the composition and organization of LH pigment-protein components in response external stimuli, such as light intensity<sup>38-40</sup>, oxygen tension,<sup>40</sup> and genetic mutation.<sup>41, 42</sup> Mimicking and expanding such responsive behavior is also highly desirable in generation of artificial light-harvesting systems. The stark difference in energy transfer observed between polymer micelles and polymer bilayer films indicates the potential of polymer composite materials for design of bioinspired, responsive photonic materials. For example, stimuli-responsive polymers integrated with chromophores have shown great potential for sensing applications,<sup>16</sup> where chromophore arrangement and FRET efficiency can be used to detect stimuli such as temperature<sup>43</sup> or pH.<sup>44</sup> Lastly, the surface patterning, selective bleaching, and use of differential chromophore mobility within our PEO-*b*-PBD films demonstrates the potential for linking polymer architecture to dynamically switchable optical properties.

In conclusion, PEO-*b*-PBD-based nanocomposites were shown to be highly versatile as a molecular framework for non-covalent incorporation of chromophores for energy transfer and light harvesting. This proof-of-concept paves the way for the investigation of other artificial LH systems based on the principle of a loosely-organized, polymer-based platform for modular component assembly. One could switch the polymer used, i.e. other diblock copolymers with desirable properties (e.g. responsive), or incorporate different hydrophobic cofactors (e.g. alternative chromophores or electron-active species). Finally, the successful exploitation of the aqueous polymer system to form supported polymer films provides attractive photonic nanomaterials for chip-based functional devices.

## **ASSOCIATED CONTENT**

### **Supporting Information**

Detailed experimental methods, characterization, analysis and theoretical modeling are given in this section. This material is available free of charge via the Internet at <http://pubs.acs.org>

## **AUTHOR INFORMATION**

### **Corresponding Authors:**

\* Email: [gbmon@lanl.gov](mailto:gbmon@lanl.gov), [shreve@unm.edu](mailto:shreve@unm.edu)

### **Author Contributions**

P.G.A. and A.M.C. contributed equally in this manuscript

### **Notes**

The authors declare no competing financial interest.

## **ACKNOWLEDGMENTS**

Experimental work by P.G.A. and Y.T. on synthesis and characterization of polymer-chromophore systems, synthesis of acceptor by T.S. and P.V., and theoretical modeling of energy transfer by V.S. and A.P.S., and SANS experiments and analysis by V.S.U. was supported by the Photosynthetic Antenna Research Center (PARC), an Energy Frontier Research Center funded by the U.S. Department of Energy, Office of Science, Basic Energy Sciences under Award # DE-SC0001035. Experimental work by A.M.C. on synthesis and characterization of polymer-chromophore systems was supported by the Laboratory Directed Research and Development (LDRD) program at Los Alamos National Laboratory (project number

20130796PRD2). Work by G.A.M. was supported by the Center for Integrated Nanotechnologies, an Office of Science User Facility operated for the U.S. Department of Energy (DOE) Office of Science. Los Alamos National Laboratory, an affirmative action equal opportunity employer, is operated by Los Alamos National Security, LLC, for the National Nuclear Security Administration of the U.S. Department of Energy under contract DE-AC52-06NA25396. Neutron scattering studies at the CG-3 Bio-SANS instrument at the High-Flux Isotope Reactor of Oak Ridge National Laboratory were sponsored by the Office of Biological and Environmental Research and by the Scientific User Facilities Division, Office of Basic Energy Sciences, U.S. Department of Energy. V.S.U. thanks K.C. Littrell at ORNL for providing SANS data reduction and analysis software.

## References

- (1) Cogdell, R. J.; Gall, A.; Koehler, J. *Q. Rev. Biophys.* **2006**, *39*, 227-324.
- (2) Gabrielsen, M.; Gardiner, A.; Cogdell, R. Peripheral Complexes of Purple Bacteria. In *The Purple Phototrophic Bacteria*; Hunter, C. N.; Daldal, F.; Thurnauer, M.; Beatty, J. T., Eds.; Springer: Dordrecht, 2009; pp 135-153.
- (3) Robert, B. Spectroscopic Properties of Antenna Complexes from Purple Bacteria. In *The Purple Phototrophic Bacteria*; Hunter, C. N.; Daldal, F.; Thurnauer, M.; Beatty, J. T., Eds.; Springer: Dordrecht, 2009; pp 199-212.
- (4) Harris, M. A.; Jiang, J.; Niedzwiedzki, D. M.; Jiao, J.; Taniguchi, M.; Kirmaier, C.; Loach, P. A.; Bocian, D. F.; Lindsey, J. S.; Holten, D.; Parkes-Loach, P. S. *Photosynth Res* **2014**, *121*, 1-14.
- (5) Harris, M. A.; Parkes-Loach, P. S.; Springer, J. W.; Jiang, J.; Martin, E. C.; Qian, P.; Jiao, J.; Niedzwiedzki, D. M.; Kirmaier, C.; Olsen, J. D.; Bocian, D. F.; Holten, D.; Hunter, C. N.; Lindsey, J. S.; Loach, P. A. *Chem. Sci.* **2013**, *4*, 3924-3933.

- (6) Springer, J. W.; Parkes-Loach, P. S.; Reddy, K. R.; Krayner, M.; Jiao, J.; Lee, G. M.; Niedzwiedzki, D. M.; Harris, M. A.; Kirmaier, C.; Bocian, D. F.; Lindsey, J. S.; Holten, D.; Loach, P. A. *J. Am. Chem. Soc.* **2012**, *134*, 4589-4599.
- (7) Anderson, J. L. R.; Armstrong, C. T.; Kodali, G.; Lichtenstein, B. R.; Watkins, D. W.; Mancini, J. A.; Boyle, A. L.; Farid, T. A.; Crump, M. P.; Moser, C. C.; Dutton, P. L. *Chem. Sci.* **2014**, *5*, 507-514.
- (8) Noy, D.; Moser, C. C.; Dutton, P. L. *Biochim. Biophys. Acta, Bioenerg.* **2006**, *1757*, 90-105.
- (9) Gust, D.; Moore, T. A.; Moore, A. L. *Acc. Chem. Res.* **2009**, *42*, 1890-1898.
- (10) Kozaki, M.; Suzuki, S.; Okada, K. *Chem. Lett.* **2013**, *42*, 1112-1118.
- (11) Bradshaw, D. S.; Andrews, D. L. *Plant Physiol.* **2011**, *3*, 2053-2077.
- (12) Mangel, M. *Biochim. Biophys. Acta, Bioenerg.* **1976**, *430*, 459-466.
- (13) Hurley, J. K.; Tollin, G. *Sol. Energy* **1982**, *28*, 187-196.
- (14) Derycke, A. S. L.; de Witte, P. A. M. *Adv. Drug Delivery Rev.* **2004**, *56*, 17-30.
- (15) Marcus, A. H.; Diachun, N. A.; Fayer, M. D. *J. Phys. Chem.* **1992**, *96*, 8930-8937.
- (16) Hu, J.; Liu, S. *Macromolecules* **2010**, *43*, 8315-8330.
- (17) Onaca, O.; Enea, R.; Hughes, D. W.; Meier, W. *Macromol. Biosci.* **2009**, *9*, 129-139.
- (18) Ma, H.; Jen, A. K. Y.; Dalton, L. R. *Adv. Mater.* **2002**, *14*, 1339-1365.
- (19) Montano, G. A.; Dattelbaum, A. M.; Wang, H. L.; Shreve, A. P. *Chem. Commun.* **2004**, 2490-2491.
- (20) Li, C.; Hu, J.; Liu, S. *Soft Matter* **2012**, *8*, 7096-7102.
- (21) Wang, R.; Peng, J.; Qiu, F.; Yang, Y. *Chem. Comm.* **2011**, *47*, 2787-2789.
- (22) Yoo, S. I.; Bae, S. H.; Kim, K.-S.; Sohn, B.-H. *Soft Matter* **2009**, *5*, 2990-2996.
- (23) Forster, S.; Berton, B.; Hentze, H. P.; Kramer, E.; Antonietti, M.; Lindner, P. *Macromolecules* **2001**, *34*, 4610-4623.
- (24) Jain, S.; Bates, F. S. *Science* **2003**, *300*, 460-464.
- (25) Pispas, S.; Hadjichristidis, N. *Langmuir* **2003**, *19*, 48-54.
- (26) Mueller, W.; Koynov, K.; Fischer, K.; Hartmann, S.; Pierrat, S.; Basche, T.; Maskos, M. *Macromolecules* **2009**, *42*, 357-361.
- (27) Goertz, M. P.; Marks, L. E.; Montaña, G. A. *ACS Nano* **2012**, *6*, 1532-1540.
- (28) El-Khouly, M. E.; Fukuzumi, S.; D'Souza, F. *ChemPhysChem* **2014**, *15*, 30-47.

- (29) Aravindu, K.; Mass, O.; Vairaprakash, P.; Springer, J. W.; Yang, E.; Niedzwiedzki, D. M.; Kirmaier, C.; Bocian, D. F.; Holten, D.; Lindsey, J. S. *Chem. Sci.* **2013**, *4*, 3459-3477.
- (30) Mortensen, K.; Brown, W.; Almdal, K.; Alami, E.; Jada, A. *Langmuir* **1997**, *13*, 3635-3645.
- (31) Lakowicz, J. R. Energy Transfer. In *Principles of Fluorescence Spectroscopy*; Springer: Dordrecht, 2006; pp 443–475.
- (32) Fung, B. K.-K.; Stryer, L. *Biochemistry* **1978**, *17*, 5241-5248.
- (33) Umena, Y.; Kawakami, K.; Shen, J.-R.; Kamiya, N. *Nature* **2011**, *473*, 55-60.
- (34) Samuilov, V. D.; Borisov, A. Y.; Barsky, E. L.; Borisova, O. F.; Kitashov, A. V. *Biochem. Mol. Biol. Int.* **1998**, *46*, 333-341.
- (35) Wrobel, D.; Graja, A. *Coord. Chem. Rev.* **2011**, *255*, 2555-2577.
- (36) Ikeda, A.; Sue, T.; Akiyama, M.; Fujioka, K.; Shigematsu, T.; Doi, Y.; Kikuchi, J.-i.; Konishi, T.; Nakajima, R. *Org. Lett.* **2008**, *10*, 4077-4080.
- (37) Calkins, J. O.; Umasankar, Y.; O'Neill, H.; Ramasamy, R. P. *Energy Environ. Sci.* **2013**, *6*, 1891-1900.
- (38) Adams, P. G.; Hunter, C. N. *Biochim. Biophys. Acta, Bioenerg.* **2012**, *1817*, 1616-1627.
- (39) Scheuring, S.; Sturgis, J. N. *Science* **2005**, *309*, 484-487,476.
- (40) Zhu, Y. S.; Hearst, J. E. *Proc. Natl. Acad. Sci. U. S. A.* **1986**, *83*, 7613-7617.
- (41) Adams, P. G.; Mothersole, D. J.; Ng, I. W.; Olsen, J. D.; Hunter, C. N. *Biochim. Biophys. Acta, Bioenerg.* **2011**, *1807*, 1044-1055.
- (42) Collins, A. M.; Liberton, M.; Jones, H. D. T.; Garcia, O. F.; Pakrasi, H. B.; Timlin, J. A. *Plant Physiol.* **2012**, *158*, 1600-1609.
- (43) Hong, S. W.; Kim, D. Y.; Lee, J. U.; Jo, W. H. *Macromolecules* **2009**, *42*, 2756-2761.
- (44) Hong, S. W.; Kim, K. H.; Huh, J.; Ahn, C.-H.; Jo, W. H. *Chem. Mater.* **2005**, *17*, 6213-6215.

# TOC

